ICAS 2021 SHANG HAI
International Council of the Aeronautical Sciences
32nd Congress of the International Council of the Aeronautical Sciences
September 6-10, 2021
Pudong Shangri-La, Shanghai, China

FLOW AND HEAT TRANSFER MECHANISM OF JET IMPINGEMENT COOLING ONTO MID-CHORD REGINE OF TWISTED BLADE

W. Jin[1], S. E. Peng[1], J. M. Wu[1]*, J. Lei[1] & W. T. Ji[2]

[1]State Key Laboratory for Strength and Vibration of Mechanical Structures
Shaanxi Key Laboratory of Environment and Control for Flight Vehicle
School of Aerospace, Xi'an Jiaotong University
Xi'an, Shaanxi, China

[2]Key Laboratory of Thermo-Fluid Science and Engineering of MOE
School of Energy and Power Engieering, Xi'an Jiaotong University
Xi'an, Shaanxi, China

*Email: wjmxjtu@mail.xjtu.edu.cn

Abstract

Jet impingement cooling is the most effective method to improve the local heat transfer coefficient. The paper numerically studied flow and heat transfer mechanism of impingement cooling onto the mid-chord region of the twisted blade with considering the thermal conductivity of the solid wall. Jet-to-jet spacing of the impingement holes are L/D_i=8 and R/D_i=6, jet-to-target spacing of the impingement holes is H/D_i=0.8, and the diameter of the impingement holes (D_i) is 0.001m. The inlet Reynolds number of mainstream is 167309, the inlet temperature of mainstream is 709K, and the pressure ratio ($P_{T,c}/ P_{T,0}$) is 1.05-1.2. The results indicate that the thermal conductivity of the blade material significantly affect the temperature distribution on the blade wall. Impingement cooling significantly reduces the temperature of the suction surface of the blade, but makes the heat transfer effect of the pressure surface worse. And the stronger the transverse flow, the worse the impingement cooling effect. Besides, the curvature of the mid-chord region of the blade also affects the impingement cooling characteristics, and the higher the pressure ratio ($P_{T,c}/ P_{T,0}$) is, the better the heat transfer effect is. Results of the study will provide some reference for the cooling design of real twisted blades.

Keywords: jet impingement; mid-chord region; twisted blade; solid material; flow heat transfer mechanism

1. Introduction

Thermal efficiency and thrust-weight ratio of modern gas turbines are constantly improved, making the inlet temperature of the turbine continue to rise. At present, the turbine inlet temperature of advanced aero engines [1] is 1800-2000K, while the highest heat resistance temperature of single crystal superalloy for blade material is 1376K, and the temperature difference is as high as more than 600 K. To ensure the safe and reliable operation of the engine at such a high temperature, both efforts on developing high-temperature resistant materials and efficient cooling techniques for turbine blade are of vital importance. Among all the heat transfer enhancement techniques, jet impingement cooling [2] is the most effective method to improve the local heat transfer coefficient in which coolant impinges on the surface of an object for convection cooling, as shown in Fig. 1. Typical usage of jet impingement in gas turbines can be found in combustor liners, leading edge, mid-chord region of turbine blade, etc. The influencing factors of impingement cooling effect have the jet hole shape, the jet array arrangement, the distance between the jet and the target plate, etc [3].

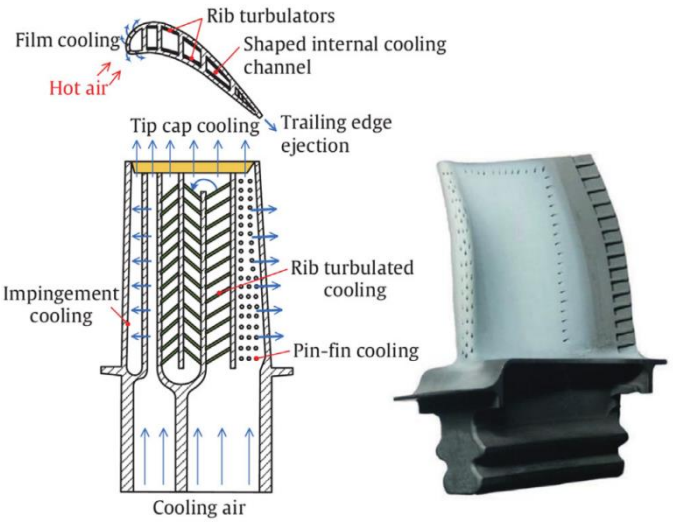

Fig. 1 Cooling techniques of turbine blade [2]

At present, the research on the jet impingement cooling has been quite extensive. The first is the leading edge cooling of the blade. The coolant is impinged through the jet hole to the leading edge and then flows out of the film hole covering the blade surface. Torres et al. [4] and Forster et al. [5] also experimentally and numerically studied the heat transfer performance of an asymmetrical-profile, leading-edge jet impingement array. Two different jet-to-target heights are tested and the range of Reynolds numbers is 20000 – 80000. The study indicated that the smaller jet-to-target height (H/d = 2.7) enhances the crossflow effects and shows better heat transfer performance. Zhang et al. [6] studied the effects of the jet hole location on the impingement cooling performance inside the leading edge of turbine blade by experimental and numerical techniques. Reynolds numbers vary from 5000 to 15000. Results indicated that different jet hole locations show different flow characteristics, resulting in different internal heat transfer. Ekkad et al. [7] experimentally explored the jet impingement cooling performance of the target plate with/without film holes. The mainstream temperature is 323K. The study found that film extraction reduces crossflow effects on jet impingement heat transfer. Zhou et al. [8] studied the effects of the film hole diameter and the location on the impingement cooling performance inside a concave target channel for the leading edge of turbine blade by numerical technique. The study does not consider the thermal conductivity of the solid wall and the Reynolds numbers vary from 10000 to 30000. Results show that film cooling hole diameter and location obviously affected the flow and heat transfer characteristics inside the target channel.

Besides, jet impingement cooling can also be applied in mid-chord region of turbine blade. Hoefler et al. [9] explored heat transfer performance of a confined impingement cooling configuration with ribs on the target surfaces by transient TLC method. Reynolds numbers vary from 10000 to 75000 and the mainstream temperature is 333K. And Chen et al. [10] also experimentally and numerically studied secondary vortex structure of a confined impingement cooling configuration with V-ribs on the target surfaces. The study does not consider the thermal conductivity of the solid wall. It is found that V-ribs enhance the secondary flow structure of the impingement cooling. Besides, Chen et al. [11] experimentally and numerically investigated the effects of different jet-to-plate spacing (H/D = 3-5), crossflow schemes, and jet Reynolds number (15,000-35,000) on the jets impingement cooling effect of a target plate with cubic micro pin fins.

To further increase the overall cooling effectiveness, double-wall cooling configuration is a very effective technique for mid-chord region of turbine blade by a narrow channel near the surface. Ji et al. [12] numerically studied the effect of jet diameters in streamwise direction on impingement cooling effect of flat plate under maximum crossflow condition (as shown in Fig. 2), and found that the configuration with increasing and then decreasing jet diameters provided higher levels of heat transfer. Stoakes et al. [13] numerically studied the effect of the diameter of impingement jets, jet-to-jet spacing, number of impingement jets, and jet-to-wall spacing, and Ramesh et al. [14] experimentally investigated the effect of the jet-to-target spacing, Reynolds number and

jet array configuration for double wall cooling applications of the flat plate. Ren et al. [15] experimentally investigated the heat transfer performance of the impingement cooling plate within a double wall cooling without considering the thermal conductivity of the solid wall. The Reynolds numbers are 96000 and 145000, and the blowing ratio vary from 4.3 to 7.3. The study found that the lower Reynolds number results in the higher adiabatic cooling effectiveness with a particular streamwise location and blowing ratio. Chen et al. [16] experimentally investigated the flow and heat transfer performance of double-wall turbine blade with integrated impingement/film and impingement/pin/film cooling configurations. The blowing ratio vary from 0.25 to 1.0. Results indicated cylindrical pins enhance the overall cooling effectiveness but reduce discharge coefficient.

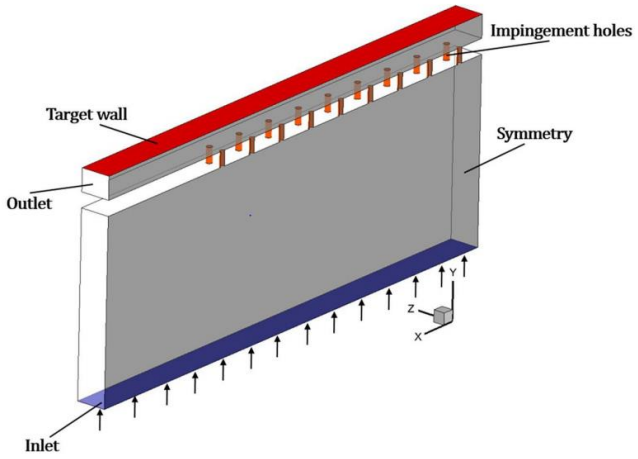

Fig. 2 Study of impingement cooling [12]

Most previous research focused primarily on the flow and heat transfer performance of a confined impingement cooling configuration with pin/rib/film on the target plate under an adiabatic condition neglecting the thermal conduction effect. However, the impingement cooling effect in the mid-chord region of turbine blade have hardly been studied. In addition, due to the small curvature in the mid-chord region of most blades, many scholars ignore the curvature of the blade and the twist in the direction of the blade height, assuming that the target surface is flat and perpendicular to the direction of the impingement jet. However, this assumption does not truly reflect the flow and heat transfer characteristics of the blade. Therefore, the paper numerically studied flow and heat transfer mechanism of impingement cooling onto the mid-chord region of the twisted blade with considering the thermal conductivity of the solid wall. Results will provide some reference for the cooling design of real turbine blades.

2. Physical Model

The paper established the simplified twisted blade model with jet impingement in the mid-chord region of the blade, as shown in Fig. 3. Figure 4 shows the blade cooling structures. The height of the blade is 0.0185m. The hydraulic diameter (D_{h0}) of the mainstream channel is 0.037m, and the hydraulic diameter (D_{hc}) of the mainstream channel is 0.01875m. To ensure the full development of the fluid at the inlet of the mainstream and internal cooling channels and avoid backflow at the outlet of the channel, the inlet and outlet channels of the computational domain are lengthened by 20 D_h respectively. Coordinate X is the flow direction of mainstream flow, coordinate Y is the direction of blade wall thickness, and coordinate Z is the height of the blade. Four rows of jet impingement holes are arranged on the suction surface of the mid-chord region of the blade, and there are three jet holes in every row, as shown in Fig. 5. Jet-to-jet spacing of the impingement holes are L/D_i=8 and R/D_i=6, jet-to-target spacing of the impingement holes is H/D_i=0.8, and the diameter of the impingement holes (D_i) is 0.001m.

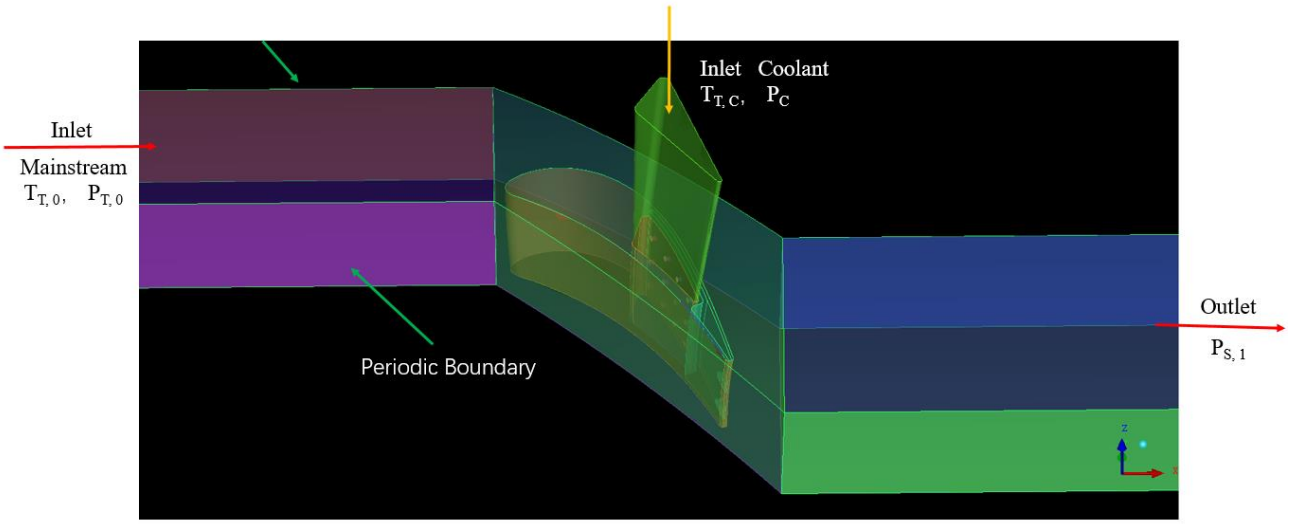

Fig. 3 Model for the present work

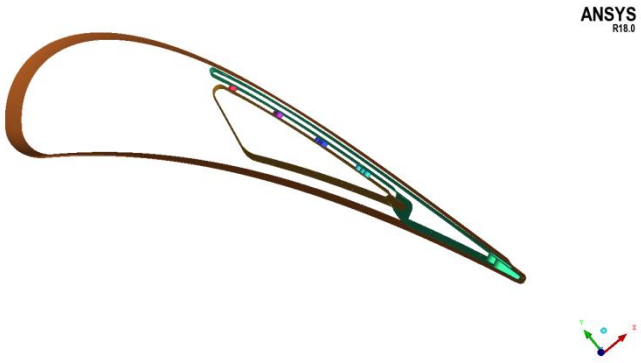

Fig.4 Blade cooling structures

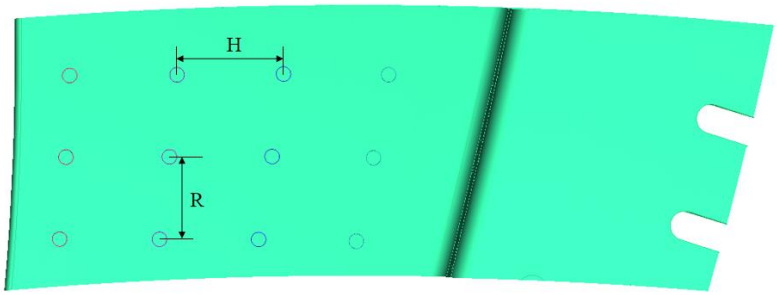

Fig. 5 Impingement holes arrangement

3. Numerical Setup

The numerical simulation is conducted with the ANSYS Fluent 18.0. The steady state simulation is done with Pressure-Velocity Coupling and the Scheme is Coupled algorithm. According to the literature [17-19], SST κ-ω turbulence model has higher accuracy to predict the flow and heat transfer performance of jet impingement cooling. Therefore, the numerical simulation is conducted with SST κ-ω turbulence model. The residual monitor of the energy equation is 10-6, the residual monitor of the continuity equation is 10-4, and other residual monitor is 10-5.

3.1 Boundary Conditions

Based on the turbine test rig from NASA [20], the inlet of the mainstream channel and coolant channel are set to be pressure-inlet boundary condition, and the outlet are set to be pressure-outlet boundary condition, as shown in Table 1. Besides, the top and bottom walls of the mainstream channel are set to be adiabatic non-slip boundary,

and two sides of the mainstream channel are rotation periodic boundary conditions. The rotation axis is the X-axis, and the rotation angle is 11.25 deg. The contacting wall between fluid and solid is set as the fluid-solid coupled surface.

Table 1 Boundary conditions

Inlet Reynolds number of mainstream (Re)	167309
Inlet total pressure of mainstream ($P_{T,0}$) / kPa	344.75
Inlet temperature of mainstream ($T_{T,0}$) / K	709
Inlet total pressure of coolant ($P_{T,c}$) / kPa	1.05 $P_{T,0}$ -1.2 $P_{T,0}$
Inlet temperature of coolant ($T_{T,c}$) / K	339
Outlet static pressure of mainstream ($P_{S,1}$) / kPa	206.437

The fluid is ideal compressible air, and specific heat, viscosity and thermal conductivity vary with temperature. As we all know, single crystal superalloy DD6 has the advantages of high temperature strength, good comprehensive performance, stable structure and good casting process performance, etc., and it is suitable for the production of high-temperature parts such as gas turbine blades with complex cavities working below 1100℃[21], which is thermal conductive, so the paper selects crystal superalloy DD6 as the solid material to account for the influence of the thermal conductivity inside the channel wall. The change of its specific heat and thermal conductivity with temperature are shown in Table 2 and Table 3.

Table 2 Specific heat of DD6

T / K	373	473	573	673	773	873	973
cp / (J/(kg•K))	358	392	427	462	196	532	566

Table 3 Thermal conductivity of DD6

T / K	293	373	473	573	673	773	873	973
k / (W/(m•K))	6.70	8.00	9.45	11.15	13.40	15.35	17.60	22.20

3.2 Definition of Feature Parameters

（1）Reynolds number in the mainstream cooling channel

$$Re = \frac{\rho u D_{h0}}{\mu} \tag{1}$$

Where ρ is air density of mainstream, kg•m^{-3}, which varies with temperature and pressure; u is the mainstream inlet velocity, m•s^{-1}; μ is air dynamic viscosity, Pa•s, which varies with temperature; D_{h0} is the hydraulic diameter of the mainstream cooling channel, m.

（2）The convective heat transfer coefficient of the blade wall

$$h = \frac{q}{T_w - T_b} \tag{2}$$

Where q is heat flux, W•m^{-2}; T_w is wall temperature on the blade, K; T_b is bulk temperature of the mainstream, K.

（3）The Nusselt number on the blade wall

$$Nu = \frac{hD_h}{k} \tag{3}$$

Where k is air thermal conductivity of mainstream, W•m^{-1}•K^{-1}， which varies with temperature.

3.3 Grid Division Method

ANSYS ICEM 18.0 is used to generate hexahedral structure grid to mesh the fluid and solid domains as detailed

in Fig. 6. Boundary layer grids are drawn around the jet impinging hole, blade surface and near all the walls of the channel for the fluid domain. The height of the first-layer of boundary layer grids is set to be small enough to satisfy the criterion that y+ value be less than 1 required by the SST κ-ω turbulence model for the current study. The grid elements number is about 11million.

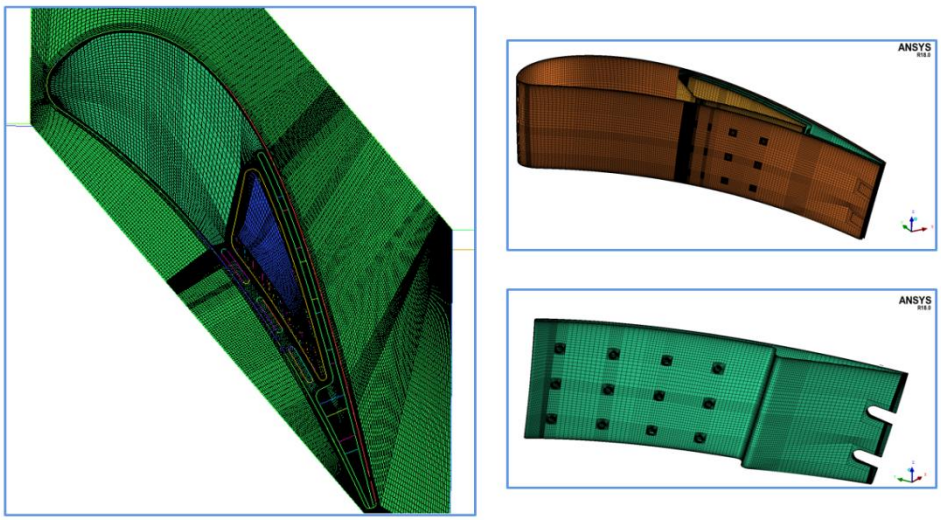

Fig. 6 Mesh of the computational domain

4. Results and Discussion

4.1 Effect of Thermal Conductivity of Solids

For turbine blade cooling under real operating conditions, the thermal conductivity of the blade material cannot be ignored. Therefore, this paper chose the actual turbine blade material (DD6) to study the effect of the thermal conductivity of solid materials on the temperature of the blade wall. The results are shown in Fig. 7. It can be found that the thermal conductivity of the solid causes the temperature of the blade wall to gradually decrease from the leading edge to the trailing edge, which enhances the heat transfer effect of the blade. At the same time, it was found that when considering the thermal conductivity of solids, the temperature of the blade wall where the impingement cavity was arranged is significantly reduced.

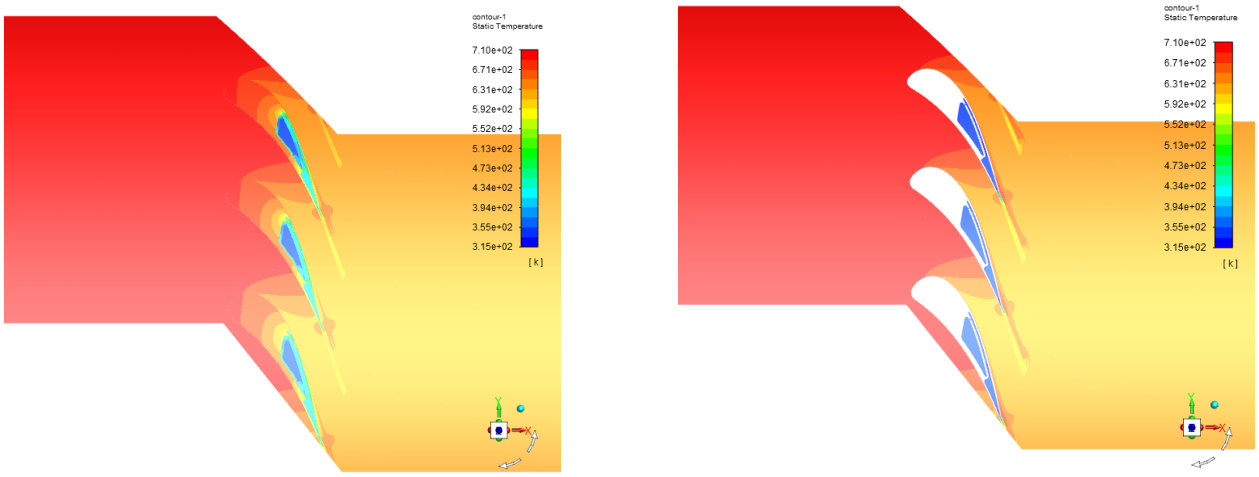

a Temperature of the middle section of blade

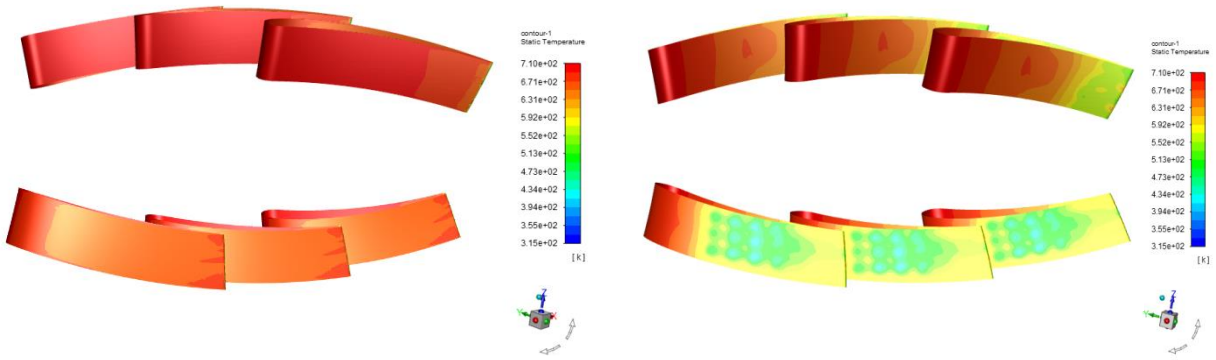

b Temperature of the blade wall

without solid with solid

Fig. 7 Temperature of the blade with / without considering the thermal conductivity of solid at $P_{T,c}$/ $P_{T,0}$=1.1

4.2 Flow Characteristics

4.2.1 Velocity Distribution

Figure 8 shows the velocity distribution of the middle section of blade, and it can be found that as the gas flows through the blade, the airflow expands and the velocity increases. This is because when the gas flows through the blade, the flow direction changes, resulting in a larger circumferential velocity component, so it has a higher velocity.

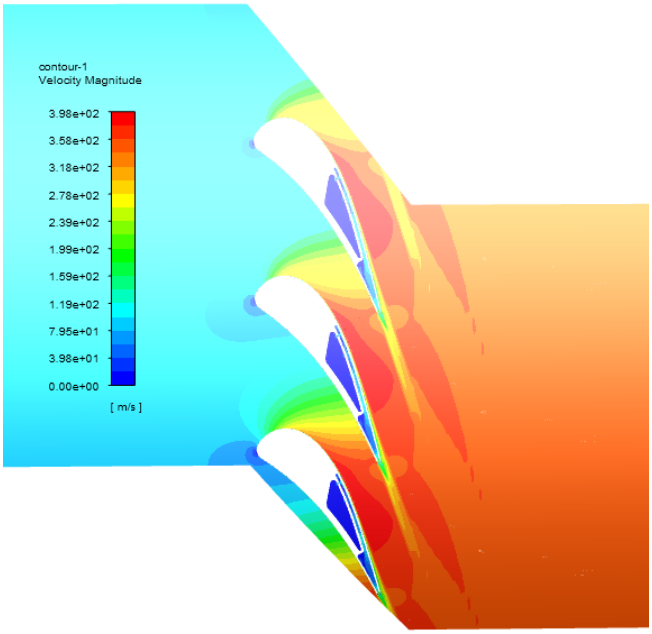

Fig. 8 Velocity vector of the middle section of blade at $P_{T,c}$/ $P_{T,0}$=1.1

The impingement channel is magnified, the flow characteristics in the impingement cooling can be observed, as shown in Fig. 9. There are two kinds of flow, transverse flow and jet flow. The jet spouts out the impingement hole and moves laterally after hitting the target surface, resulting in transverse flow, which will change the flow characteristics of the adjacent jet flow. It can be seen from Fig. 9 that on the same cross section, due to the curvature of the blades, the outflow and entry directions of the transverse flow are different, and the strength is also different. The transverse flow makes the jet deviate from the impingement position, although the convective heat transfer is enhanced, but the jet deviates, thereby weakening the impingement cooling effect. Therefore, the impingement cooling effect is poor in locations with strong transverse flow, such as the last row of impingement holes. Z=0.271m and z=0.2654m respectively correspond to the two cross sections of the blade with impingement holes. Comparing the flow in the impingement channel on the two cross-sections, it is found that because the paper is studying a twisted blade, the transverse flow generated in the same row of impingement holes on different cross sections is also different. It can be seen that when studying impingement cooling, the transverse flow has a great influence on impingement cooling. At the same time, the mid-chord region of the blade cannot be simplified to a plane, because the curvature of the blade also affects the impingement cooling effect.

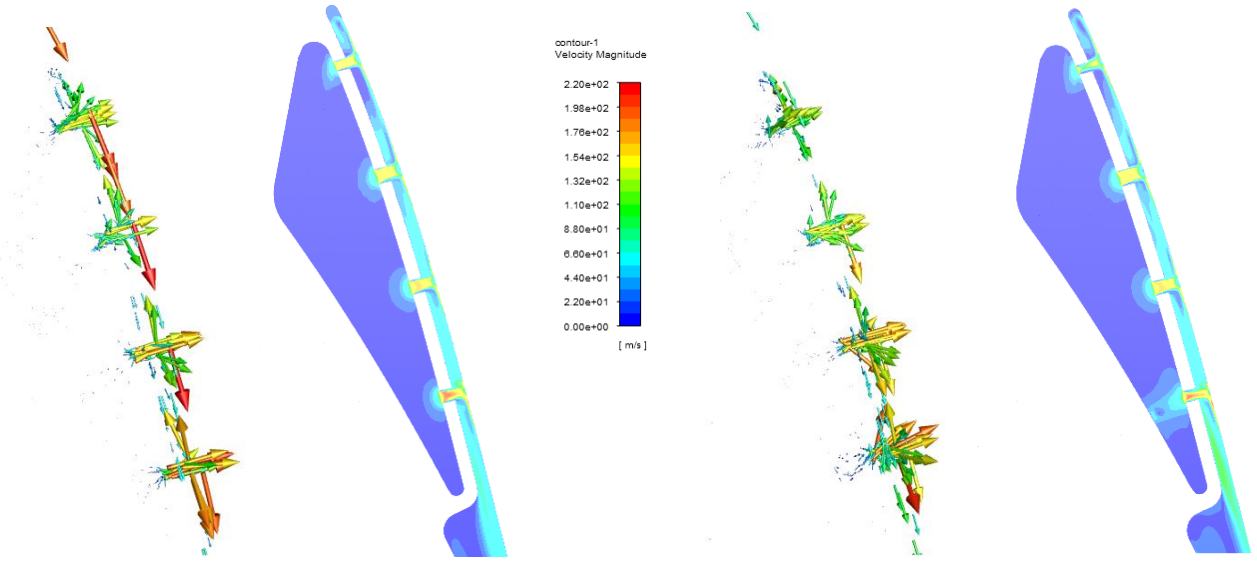

z=0.271m z=0.2654m

Fig. 9 Velocity distribution of the cross section in the direction of blade height at $P_{T,c}/ P_{T,0}$=1.1

4.3 Heat transfer Characteristics

Figure 10 shows the temperature of the blade with / without the impingement cooling at $P_{T,c}/ P_{T,0}$=1.1. It can be found that impingement cooling significantly reduces the temperature of the suction surface of the blade, but makes the heat transfer effect of the pressure surface worse. This is because after the cooling cavity is arranged on the suction surface, the coolant is distributed unevenly in the internal cooling channel, and all coolant flows out from the impingement hole on the suction surface, which enhances the heat transfer in the region near the impingement hole on the suction surface, but weakens the heat transfer effect on the pressure surface. From the Nussel number curve of the middle section of the blade, it can be found that the Nussel number of the position where the impingement hole is arranged increases significantly, corresponding to four peaks in the Fig. 11. At the same time, it can be seen that the Nussel number of each row of impingement holes is different, because the coolant is not evenly distributed in the internal cooling channel and the curvature of the target surface is different, so that the transverse flow intensity of each row of impingement holes is different, resulting in different heat transfer effects, as shown in Fig. 9 and Fig. 11. In addition, the paper also compares the heat transfer effect on the different cross sections of the blade, as shown in Fig. 12 and Fig. 13. It can be found that the impingement cooling effect at the cross section z=0.2596m is the best. The impingement cooling effect at the cross section Z =0.271m is the worst. This is because, with the flow of coolant, the intensity of transverse flow is gradually weakened (as shown in Fig. 9), and the heat transfer capacity is gradually enhanced. At the same time, the third row of impingement holes has the best heat transfer effect, and that of the first row of impact holes is worst at $P_{T,c}/ P_{T,0}$=1.1. Figure 14 shows the averaged Nusselt number on the blade wall. It can be found that the averaged Nusselt number of Case1 is 1.23-1.25 times that of Base Case.

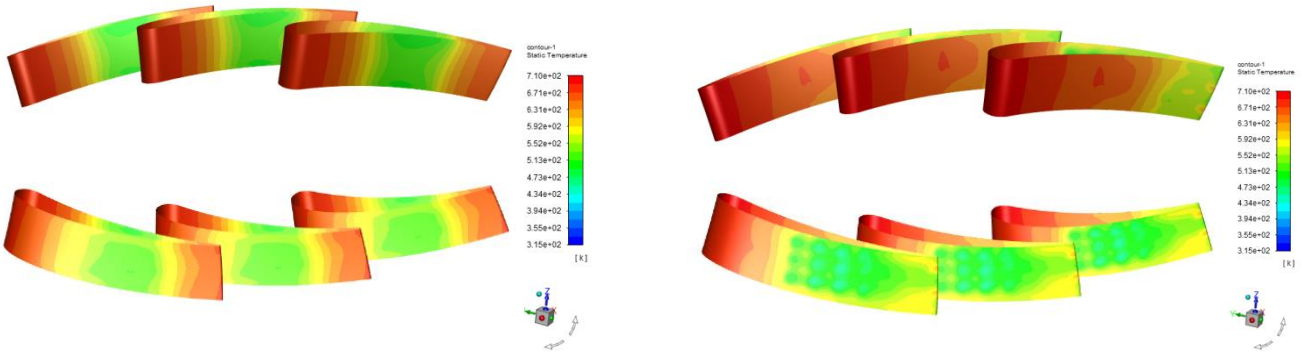

without the impingement cooling (Base Case) with the impingement cooling (Case1)

Fig. 10 Temperature of the blade with / without the impingement cooling at $P_{T,c}/ P_{T,0}$=1.1

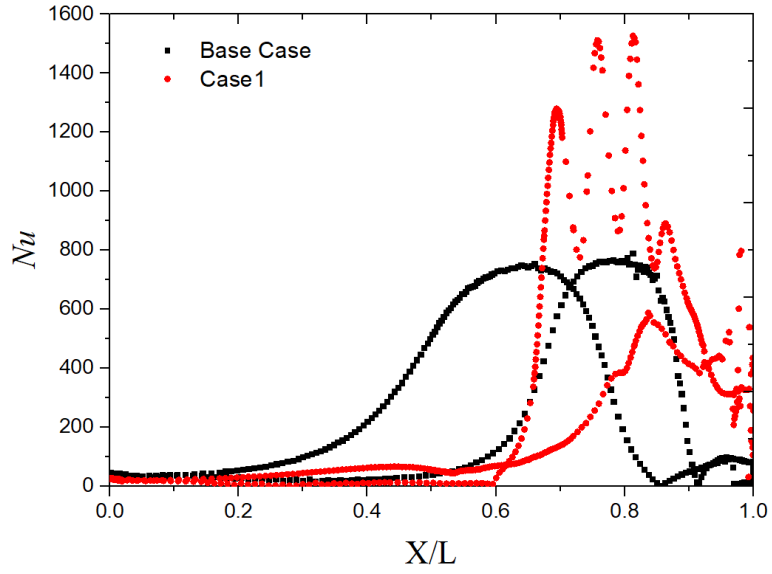

Fig. 11 Nusselt number on the middle section of the blade at $P_{T,c}/ P_{T,0}$=1.1

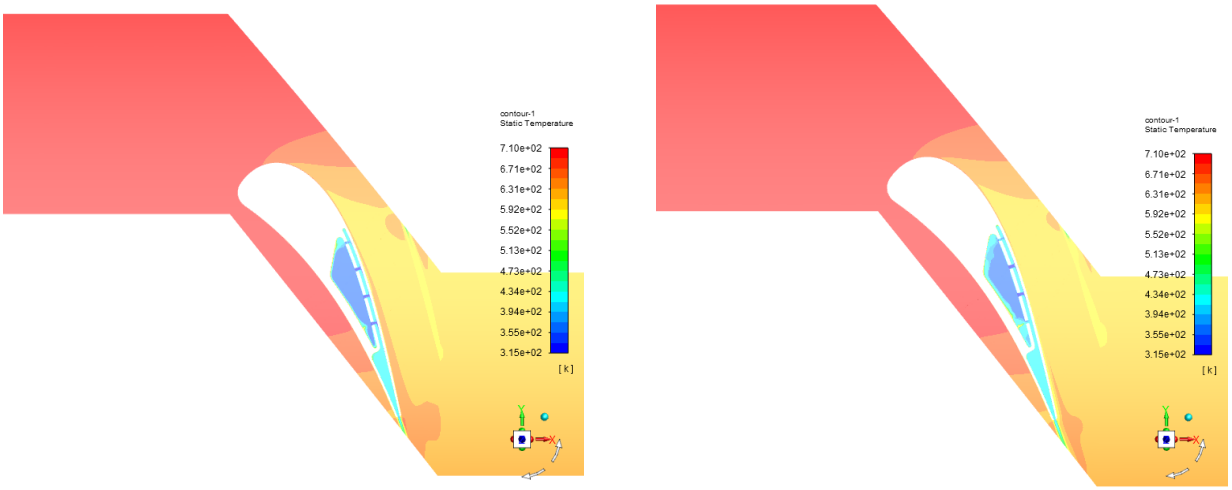

z=0.271m z=0.2654m

Fig. 12 Temperature of the middle section of blade

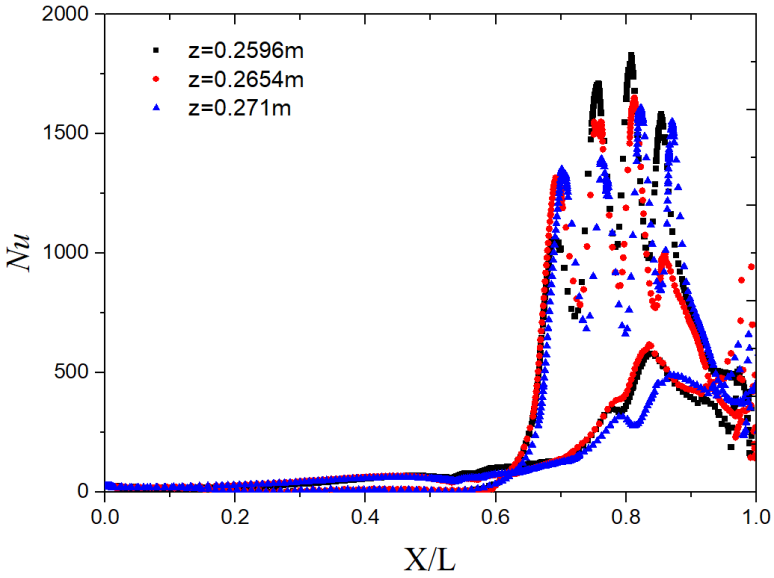

Fig. 13 Nusselt number on the cross section of the blade at $P_{T,c}/ P_{T,0}$=1.1

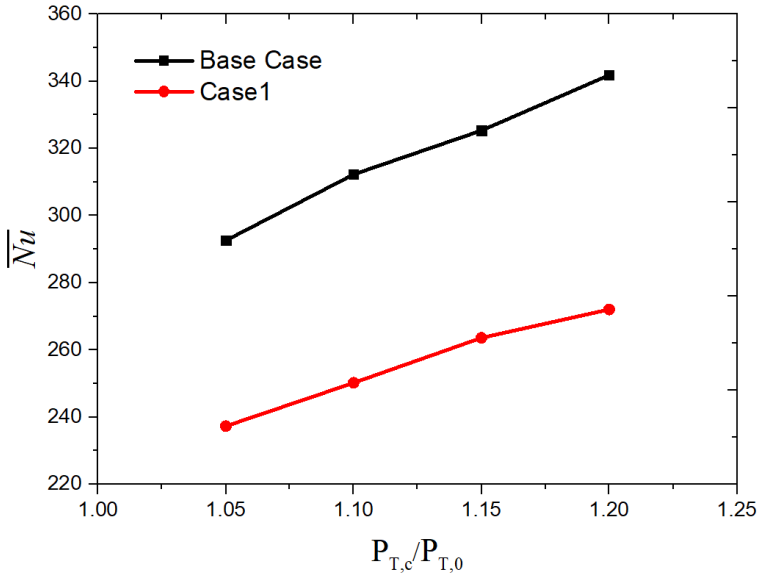

Fig. 14 Averaged Nusselt number on the blade wall

4.4 Effect of $P_{T,c}/ P_{T,0}$

Figure 15 shows the temperature of the blade at different $P_{T,c}/ P_{T,0}$. It can be found that the higher the pressure ratio ($P_{T,c}/ P_{T,0}$) is, the lower the temperature of the blade, and the better the heat transfer effect is, as shown in Fig.16. Because the larger the pressure ratio ($P_{T,c}/ P_{T,0}$) is, the larger the ratio between the mass flux of the jet hole and the transverse flow flux is, resulting in the influence of the transverse flow on the deviation of the jet flow is smaller, the heat transfer effect is better. At the same time, the larger the pressure ratio ($P_{T,c}/ P_{T,0}$), the larger the mass flux of the jet hole, the greater the jet velocity, the stronger the jet impingement on the target surface, and the better the heat transfer effect.

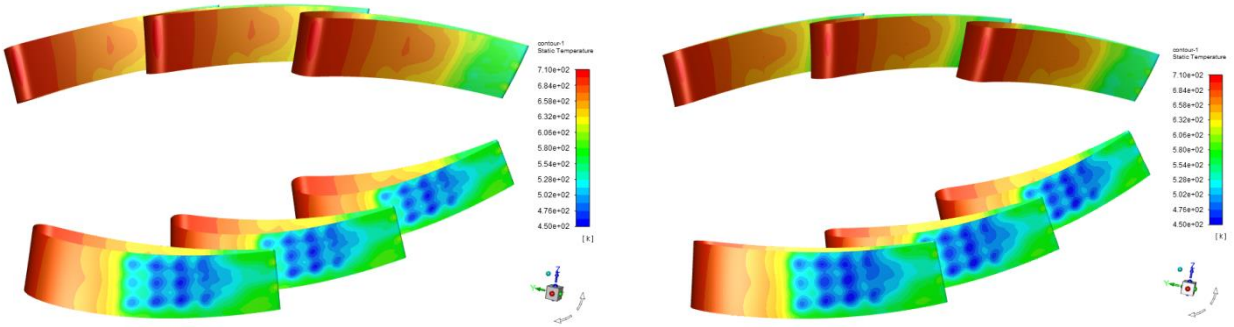

$P_{T,c}/ P_{T,0}$=1.1 $P_{T,c}/ P_{T,0}$=1.2

Fig. 15 Temperature of the blade at different $P_{T,c}/ P_{T,0}$

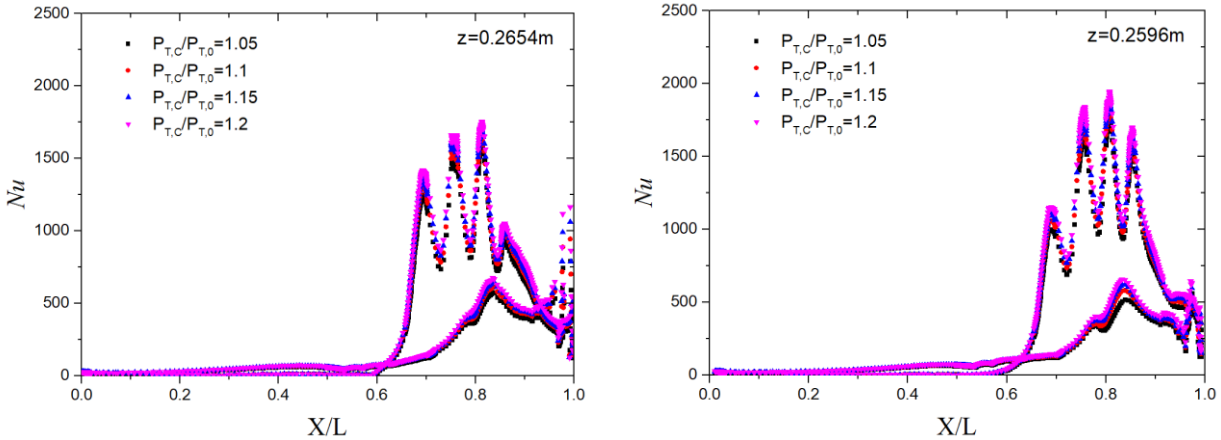

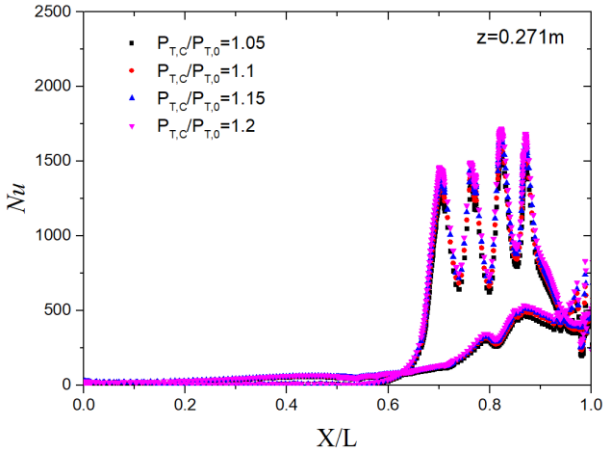

Fig. 16 Nusselt number on the cross section of the blade at different $P_{T,c}/ P_{T,0}$

5. Conclusions

The paper numerically studied flow and heat transfer mechanism of impingement cooling onto the mid-chord region of the twisted blade with considering the thermal conductivity of the solid wall. The conclusions are as follows:

(1) The thermal conductivity of the blade material significantly affect the temperature distribution on the blade wall.

(2) Transverse flow weakens the impingement cooling effect.

(3) The mid-chord region of the blade cannot be simplified to a plane, because the curvature of the blade also affects the impingement cooling effect.

(4) Impingement cooling significantly reduces the temperature of the suction surface of the blade, but makes the heat transfer effect of the pressure surface worse.

(5) High pressure ratio ($P_{T,c}/ P_{T,0)}$ will enhance the heat transfer effect of the blade.

6. Acknowledgments

The work is supported by the National Science and Technology Major Project （2017-lll-0003-0027).

7. Copyright Statement

References

[1] Walsh PP, and Fletcher P. *Gas turbine performance.* 2nd ed, 2004.

[2] Kaewchoothong N, Maliwan K, Takeishi K, and Nuntadusit C. Effect of inclined ribs on heat transfer coefficient in stationary square channel. *Theoretical and Applied Mechanics Letters*, vol. 7, no. 6, pp. 344-350, 2017. DOI: 10.1016/j.taml.2017.09.013.

[3] Han J C, Dutta S, and Ekkad S. *Gas turbine heat transfer and cooling technology*. New York: Taylor&Francis, 2000.

[4] Torres J, Husam Z, Erik F, Jayanta K, and Jose R. Experimental and numerical study of array jet impingement cooling on a leading-edge curved surface. ASME Paper No. GT2020-14810, 2020. DOI: 10.1115/GT2020-14810.

[5] Forster M, and Weigand B. Experimental and numerical investigation of jet impingement cooling onto a concave leading edge of a generic gas turbine blade. *International Journal of Thermal Sciences*, Vol. 164, 2021. DOI: 10.1016/j.ijthermalsci.2021.106862.

[6] Zhang MJ, Wang N, and Han JC. Internal heat transfer of film-cooled leading edge model with normal and tangential impinging jets. *International Journal of Heat and Mass Transfer*, Vol. 139, pp. 193-204, 2019. DOI: 10.1016/j.ijheatmasstransfer.2019.04.140.

[7] Ekkad SV, Huang YZ, and Han JC. Influences of effusion hole diameter on impingement/effusion cooling performance at turbine blade leading edge. *Journal of Thermophysics and Heat Transfer*, Vol. 13, No. 4, pp. 522-528, 1999. DOI: 10.2514/2.6471.

[8] Zhou JF, Wang XJ, and Li J. Influences of effusion hole diameter on impingement/effusion cooling performance at turbine blade leading edge. *International Journal of Heat and Mass Transfer*, Vol. 134, pp. 1101-1118, 2019. DOI: 10.1016/j.ijheatmasstransfer.2019.02.054.

[9] Hoefler F, Schueren S, and von Wolfersdorf J. Heat Transfer Characteristics of an Oblique Jet Impingement Configuration in a Passage With Ribbed Surfaces. *Journal of Turbomachinery-Transactions of the ASME*, Vol. 134, No. 3, p. 031022, 2012. DOI: 10.1115/1.4003084.

[10] Chen LL, Brakmann RGA, Weigand B, Rodriguez J, Crawford M, and Poser R. Experimental and numerical heat transfer investigation of an impingement jet array with V-ribs on the target plate and on the impingement plate. *International Journal of Heat and Fluid Flow*, Vol. 68, pp. 126-138, 2017. DOI: 10.1016/j.ijheatfluidflow.2017.09.005.

[11] Brakmann R, Chen LL, Weigand B, Rodriguez J, and Crawford M. Experimental and Numerical Heat Transfer Investigation of an Impinging Jet Array on a Target Plate Roughened by Cubic Micro Pin Fins. *Journal of Turbomachinery-Transactions of the ASME*, Vol. 138, No. 11, p. 111010, 2016. DOI: 10.1115/1.4033670.

[12] Ji YB, Singh P, Ekkad SV, and Zang SS. Effect of crossflow regulation by varying jet diameters in streamwise direction on jet impingement heat transfer under maximum crossflow condition. N*umerical Heat Transfer Part A-Applications*, Vol. 72, No. 8, pp. 579-599, 2017. DOI: 10.1080/10407782.2017.1394136.

[13] Stoakes P, and Ekkad S. Optimized impingement configurations for double wall cooling applications. ASME Paper No. GT2011-46143, 2011. DOI: 10.1115/GT2011-46143.

[14] Ramesh S, Narzary D and Ekkad SV. Optimization of low jet-to-target spacing ratio for double wall impingement cooling applications. AIAA Paper No. AIAA 2012-0367, 2012. DOI: 10.2514/6.2012-367.

[15] Ren Z, Vanga SR, Rogers N, Ligrani P, Hollingsworth K, Liberatore F, Patel R, Srinivasan R and Ho YH. Internal and external cooling of a full coverage effusion cooling plate: Effects of double wall configuration and conditions. *International Journal of Thermal Sciences*, Vol. 124, pp. 36-49, 2017. DOI: 10.1016/j.ijthermalsci.2017.09.021.

[16] Chen Y, Wei H, and Zu YQ. Experimental study on the conjugate heat transfer of double-wall turbine blade components with/without pins. *Thermal Science and Engineering Progress*, Vol. 8, pp. 448-456, 2018. DOI: 10.1016/j.tsep.2018.09.010.

[17] Zuckerman N, and Lior N. Jet impingement heat transfer: Physics, correlations, and numerical modeling. *Advances in Heat Transfer*, Vol. 39, pp. 565–631, 2006. DOI: 10.1016/S0065-2717(06)39006-5.

[18] Dutta R, Dewan A, and Srinivasan B. Comparison of various integration to wall (ITW) RANS models for predicting turbulent slot jet impingement heat transfer. *International Journal of Heat and Mass Transfer*, Vol. 65, pp. 750–764, 2013. DOI: 10.1016/j.ijheatmasstransfer.2013.06.056.

[19] Fechter S, Terzis A, Ott P, Weigand B, von Wolfersdorf J, and Cochet M. Experimental and numerical investigation of narrow impingement cooling channels. *International Journal of Heat and Mass Transfer*, Vol. 67, pp. 1208–12192013. DOI: 10.1016/j.ijheatmasstransfer.2013.09.003.

[20] Timko LP. Energy efficient engine high pressure turbine component test performance report. *National Aeronautics and Space Administration*, NASA CR-168289, 2017.

[21] *China aeronautical materials handbook*, Bei Jing, Second Edition, 2001.